



IMPLEMENTATION AND VERIFICATION OF SHEAR TRANSFER MECHANISM MODULE OF REINFORCED CONCRETE

Hideaki Sonobe¹, Wataru Hotta², Shunichi Suzuki³, Hiroki Motoyama⁴ and Muneo Hori⁵

¹ Chief, Taisei Corporation, Tokyo, Japan (snbhda00@pub.taisei.co.jp)

² Manager, Taisei Corporation, Tokyo, Japan

³ Deputy Director, Taisei Corporation, Tokyo, Japan

⁴ Associate Professor, National Defense Academy of Japan, Kanagawa, Japan

⁵ Director-General, Japan Agency for Marine-Earth Science and Technology, Kanagawa, Japan

ABSTRACT

The shear transfer mechanism of multiple cracked concrete is a major difficulty of nonlinear seismic response analysis to examine the ultimate capacity of a reinforced concrete (RC) reactor building subjected to extremely strong ground motion. In this study, we implement a module for the shear transfer mechanism to the parallel finite element method that is developed to analyse a high-fidelity model. The module ought to be applicable to various patterns of multiple cracking that is induced by cyclic loading of ground motion and is required to make stable numerical computation which is caused by abrupt changes of shear stiffness when the crack state transform among loading, unloading, and reloading. It is shown that the implemented module is applicable to all patterns of multiple cracking for two cracks. A numerical experiment of shear walls is carried out to examine the performance of the developed module.

INTRODUCTION

Since the 2011 Tohoku Earthquake, design earthquake ground motion has increased in Japan, and new methods to evaluate seismic responses of a nuclear power plant have been developed. A large-scale computing method is developed to take advantage of high-performance computing technology so that a three-dimensional high-fidelity model of a few million degree-of-freedom can be analysed. The two merits of the large-scale computing method are a wider range of applicability to larger seismic loads and a higher spatial and temporal resolution of the numerical analysis. A general-purpose parallel finite element method, called E-FrontISTR, has been developed by implementing modules which are required for the seismic structural response analysis to an open-source structural analysis solver, FrontISTR. The developed program has demonstrated sufficient resolution and accuracy for practical use and sufficient computational performance.

To evaluate seismic response analysis for extremely strong ground motions, it is necessary to compute the effects of multi-directional inputs on the local damages of concrete members which are modelled as multiple cracking. Due to the presence of reinforcement, each crack transfers shear stress on its surface. As the number of cracking increases, accurate evaluation of transferred shear stress becomes more difficult; the amount of shear stress depends on the three states, called loading, unloading, and reloading, which correspond to the increase of inelastic deformation, the decrease of inelastic deformation, and the increase of inelastic deformation before the previous maximum inelastic deformation.

In this paper, we focus on the development of a new module for the shear transfer mechanism of multiple cracked concrete, which is proposed by Maekawa et al. The following two are the key issues of the development: 1) overcoming of unrealistically large shear stiffness at the beginning of cracking; and 2) the general applicability of analysing multiple cracking of any arbitrary crack plane orientations. The developed module was implemented into E-FrontISTR, and numerical experiments were carried for the verification; all patterns of multiple-cracking were tested and the transition among the three states of loading, unloading, and reloading was studied.

OVERVIEW OF THE SHEAR TRANSFER MODEL FOR REINFORCED CONCRETE

Shear Transfer Model Proposed by Maekawa et. al

The shear transfer constitutive relation proposed by Maekawa is expressed in terms of shear stress-shear strain relation, as follows:

$$\tau_{st}(\beta) = \begin{cases} f_{st} \frac{\beta^2}{1+\beta^2} & (\beta \geq \beta_{max}) \\ \frac{\tau_{max}}{0.15\beta_{max}} (\beta - 0.85\beta_{max}) & (\beta_{max} > \beta \geq 0.9\beta_{max}), \\ \frac{1}{3} \tau_{max} \left(\frac{\beta}{0.9\beta_{max}} \right)^9 & (0.9\beta_{max} > \beta > 0.0) \end{cases} \quad (1)$$

where

$$\beta = \frac{\gamma_{cr}}{\varepsilon_t} \quad (2)$$

is normalized shear strain with shear strain due to crack γ_{cr} and tensile strain normal to crack ε_t ; β_{max} and τ_{max} are the past maximum value of β and τ_{st} , and f_{st} is shear transfer strength.

Maekawa et al.⁵⁾ proposed an explicit equation to distribute shear strain to each crack for an orthogonal two-direction cracking condition, accounting for the interaction of the two cracks; see Fig. 1. The equation for the shear strain distribution is written in the following form:

$$\begin{cases} \tau_{st}(\beta_1) = \tau_{st}(\beta_2) \\ \gamma_{cr1} + \gamma_{cr2} = \gamma \end{cases}, \quad (3)$$

where β_1 and β_2 are normalized shear strain for the 1st and 2nd cracks, γ_{cr1} and γ_{cr2} are the shear strain due to the 1st and 2nd crack, and γ is total shear strain. Equation (3) is solved in an iterative manner in the numerical analysis. As shown in Eq. (1), a polynomial of 9th order is used for the case of $0.9\beta_{max} > \beta > 0.0$, which will be hinge for the iterative analysis.

Maekawa et al. presented a simplified shear transfer constitutive relation expressed as

$$\tau_{st}^*(\beta) = \begin{cases} f_{st} \frac{\beta^2}{1+\beta^2} & (\beta \geq \beta_{max}) \\ \frac{\tau_{max}}{0.15\beta_{max}} (\beta - 0.85\beta_{max}) & (\beta_{max} > \beta \geq 0.85\beta_{max}). \\ 0 & (0.85\beta_{max} > \beta > 0.0) \end{cases} \quad (4)$$

Equation (3) is then replaced by

$$\begin{cases} \tau_{st}^*(\beta_1) = \tau_{st}^*(\beta_2) \\ \gamma_{cr1} + \gamma_{cr2} = \gamma \end{cases}, \quad (5)$$

which can be solved much more easily in the numerical analysis.

The distribution of shear strain on each crack changes depending on the state of each crack, i.e., loading, unloading or reloading; these three states are designated by (A), (B) or (C), respectively, in Fig. 1. It should be noted that each crack has two internal state variables, the past maximum shear stress and normalized shear strain denoted by τ_{max} and β_{max} . For instance, if the 1st crack experiences shear damage before the 2nd crack, these internal state variables satisfy $\tau_{max1} > \tau_{max2}$ and $\beta_{max1} > \beta_{max2}$, where subscript 1 or 2 stands for the internal state variables of the 1st or 2nd crack, respectively.

Module for Shear Stress Transfer Mechanism

In E-FrontISTR, the element shear stress, denoted by τ , is calculated for the element shear strain, denoted by γ , as follows:

$$\tau = G\gamma, \quad (6)$$

where G is the element shear stiffness. For each crack, shear stress and shear strain, denoted by τ_{st} and γ_{cr} , are related through

$$\tau_{st}(\beta) = G_{cr}\gamma_{cr}, \quad (7)$$

where G_{cr} is the shear stiffness of the crack. This $\tau_{st}(\beta)$ is required to satisfy $\tau_{st}(\beta) = \tau$.

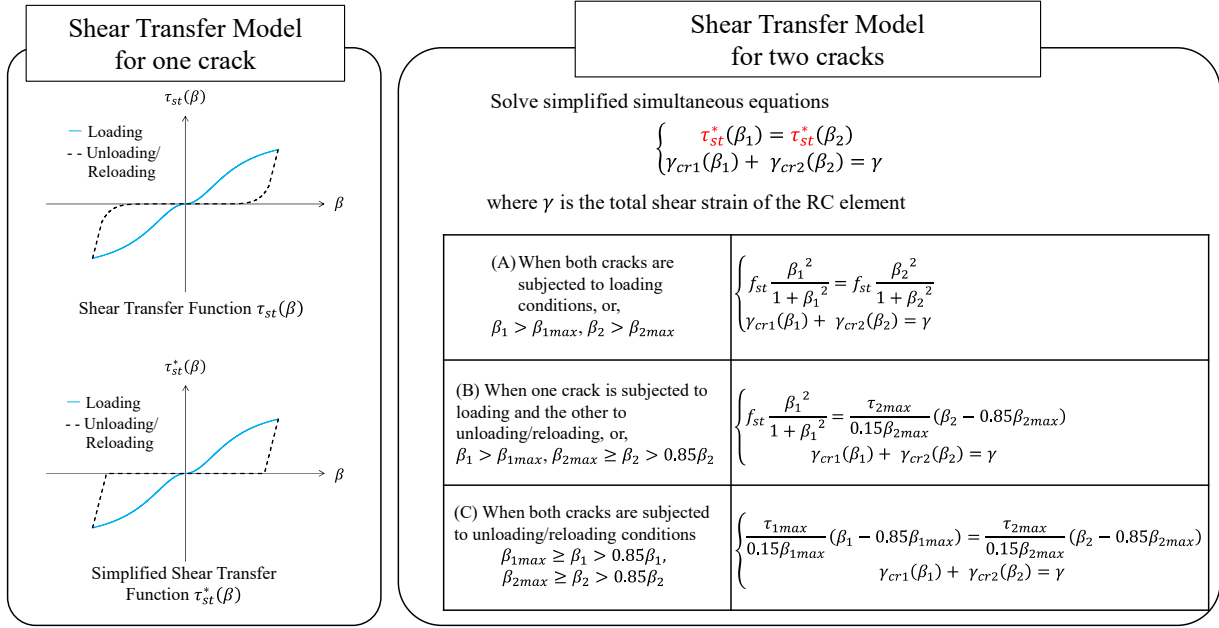


Figure 1. Shear transfer mechanism proposed by Maekawa et. al.

E-FrontISTR assumes element shear stress equals crack shear stress, while element shear strain is distributed to crack shear strain. The same assumption is employed by another general purpose finite element method¹⁾. It should be emphasized that E-FrontISTR account for the interaction effects between multiple cracks by distributing the element shear strain; the shear stress-shear strain relation is not changed for interacting multiple cracks.

When tensile strain is small, normalized shear strain defined by Eq. (2) and hence the shear stiffness of crack, i.e., G_{cr} , becomes large. This sometimes leads to unstable numerical computation because some components of the global stiffness matrix become too large due to large G_{cr} ; E-FrontISTR employs an iterative solver based on the conjugate gradient method which does not provide a converged solution for an ill-natured matrix.

Maekawa et. al.^{2), 5)} has developed an RC structure analysis program called COM3. In COM3, the element shear stiffness shown in Eq. (6) is computed as

$$G = \left(\frac{1}{G_c} + \frac{1}{G_{cr}} \right)^{-1}, \quad (8)$$

where G_c is uncracked concrete stiffness and G_{cr} is defined as

$$G_{cr} = \frac{\tau_{st}(\beta)}{\gamma_{cr}}; \quad (9)$$

note that $\tau_{st}(\beta)$ is given by Eq. (1). For the case of two cracks, G is computed as

$$G = \left(\frac{1}{G_c} + \frac{1}{G_{cr1}} + \frac{1}{G_{cr2}} \right)^{-1}, \quad (10)$$

where G_{cr1} and G_{cr2} are defined for the 1st and 2nd crack according to Eq. (9).

NUMERICAL EXPERIMENTS OF SHEAR TRANSFER MECHANISM MODULE

We conducted comparative numerical experiments of a single element model subjected to shear loading, using E-FrontISTR implemented with the developed module for shear transfer mechanism. The experiment followed the reference³⁾, where tensile force was loaded to a concrete element to be cracked orthogonally, and then shear force was loaded. Figure 2 shows the element and the coordinates; the crack planes are normal to the X-axis and Z-axis.

We first used E-FrontISTR onto which the developed module was not implemented. The relation between the shear strain and stress in the loading direction is shown in Fig. 2, too; the computed relation and the relation shown in the reference are designated by blue and black lines, respectively. As is seen, E-FrontISTR evaluates shear stress higher than the reference. This is because the stiffness of uncracked concrete stiffness is not considered, and Eq. (8) or (10) is not used for the element shear stiffness in the old E-FrontISTR.

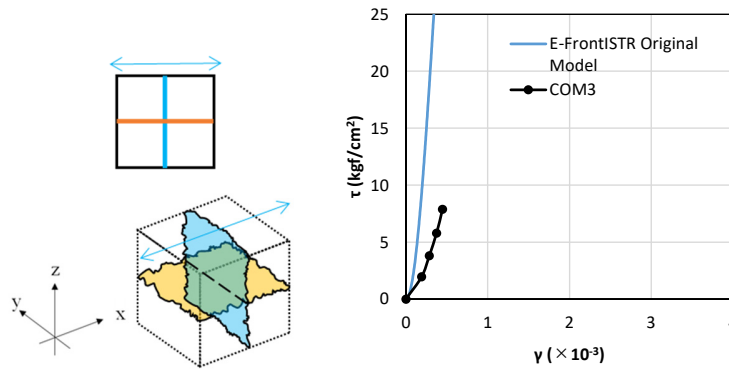


Figure 2. Comparative analysis of old E-FrontISTR with COM3.

Now, we verify the developed module for the shear transfer mechanism. The difficulty in the numerical analysis lies for complicated loading conditions which induce multiple cracking. As shown in Fig. 1, there are the following three cases of the loading states of two crack planes: 1) the loading state for both crack planes; 2) the loading state for one crack plane and the unloading/reloading state for another; and 3) the unloading/reloading state for the both crack planes. Considering the order of cracking, there are eight patterns of two cracks as shown in Fig. 3.

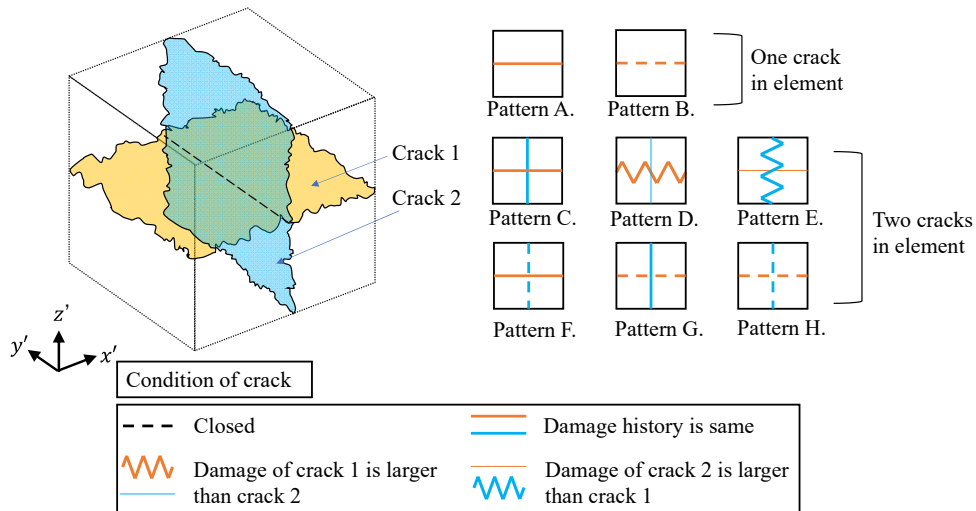


Figure 3. Eight patterns of crack state for two crack planes.

As shown in Fig. 3, Patterns D and E corresponds to the case where one crack is much more damaged than the other. This often happens when the loading that induces the first crack is large, leaving the

second crack small. For these patterns, we made a special treatment in the module. Since these patterns correspond to the second case shown in Fig. 1, we derive the following equation:

$$\begin{cases} D \gamma_{cr1}^3(\beta_1) + C \gamma_{cr1}^2(\beta_1) + B \gamma_{cr1}(\beta_1) + A = 0 \\ \gamma_{cr2}(\beta_2) = \gamma - \gamma_{cr1}(\beta_1) \end{cases}, \quad (11)$$

where β_1 is the normalized shear strain of the loading state crack and β_2 is the normalized shear strain for the unloading/reloading crack; A , B , C and D are constants.

It should be noted that for Patterns D and E, β_1 and β_2 must satisfy

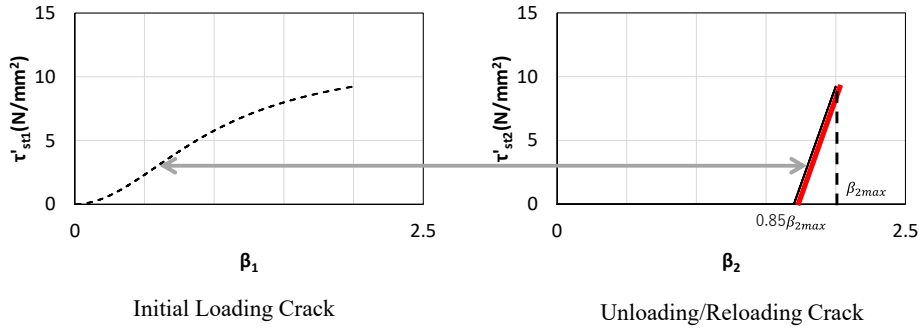
$$\beta_1 \geq \beta_{1max}, \beta_{2max} > \beta_2 \geq 0.85 * \beta_{2max}. \quad (12)$$

If element shear strain γ is so small so that β_2 violates the second equation of Eq. (11), i.e., $\beta_2 < 0.85 * \beta_{2max}$, there will be no solution for Eq. (11). For this case of small γ , the module prepared an alternative solution which is used during a brief period of small γ as

$$\beta_1 = 0, \beta_2 = \frac{\gamma}{\varepsilon_{t2}}. \quad (13)$$

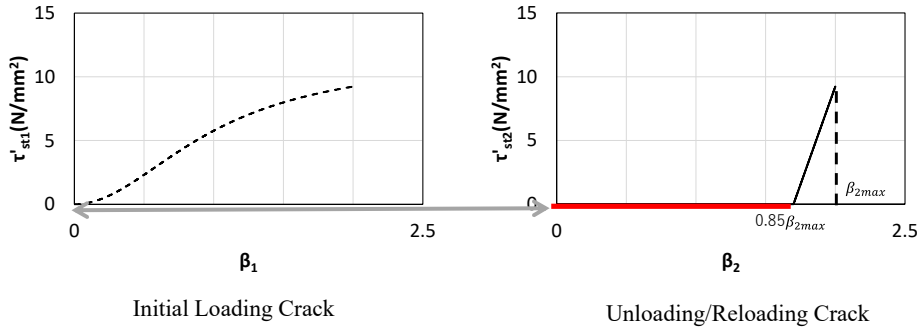
An illustration for this alternative solution is presented in Fig. 4.

- When $\beta_{2max} > \frac{\gamma_{cr2}}{\varepsilon_{t2}} \geq 0.85 * \beta_{2max}$



$$\beta_1, \beta_2 \text{ exists that satisfy } \tau'_{st1}(\beta_1) = \tau'_{st1}(\beta_2)$$

- When $0.85 \beta_{2max} > \frac{\gamma_{cr2}}{\varepsilon_{t2}}$



$$\text{No } \beta_1, \beta_2 \text{ exists that satisfy } \tau'_{st1}(\beta_1) = \tau'_{st1}(\beta_2)$$

The solution is simplified as $\beta_1=0, \beta_2 = \frac{\gamma}{\varepsilon_{t2}}$, or $\gamma_{cr1} = 0, \gamma_{cr2} = \gamma$, and $\tau'_{st1}(\beta_1) = \tau'_{st1}(\beta_2) = 0$

Figure 4. Process of solving the cubic equation.

We conducted numerical experiments of a single element model to verify the developed module for all the eight patterns of the crack states of two crack planes, which are shown in Fig. 3. The loading conditions and the resulting shear strain-shear stress relation are presented in Fig. 5; five loading conditions are used to realize the patterns. Pattern B. and Pattern H. are cracked elements but the cracks are reclosed, so it works the same as an uncracked element. Pattern F. and G. are symmetrical. So checking the Patterns A., C., D., E. and G. are sufficient for Fig 5.

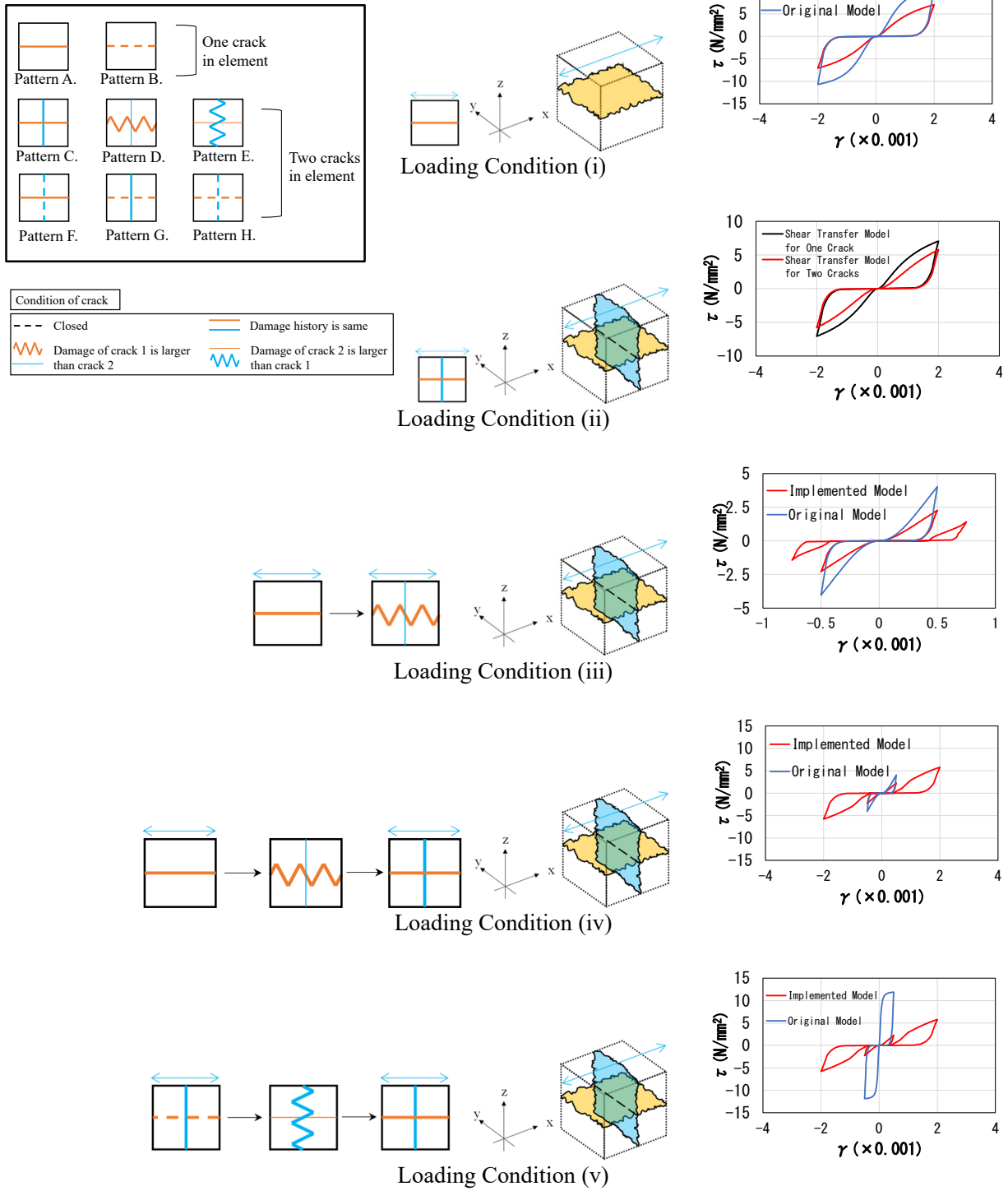


Figure 5. Verification tests of module of shear transfer mechanism.

For Loading Conditions (i) and (ii), which correspond to Patterns A and C, respectively, we check the improvement of using Eq. (8) and (10). It was shown that the module succeeds to decrease the shear stress.

For Loading Conditions (iii) and (iv), which correspond to Pattern D, two loops of cyclic shear loading are applied; the range of shear strain is $-0.5 \cdot 10^{-3} \leq \gamma \leq 0.5 \cdot 10^{-3}$ in the first loop and is $-0.75 \cdot 10^{-3} \leq \gamma \leq 0.75 \cdot 10^{-3}$ and $-2.0 \cdot 10^{-3} \leq \gamma \leq 2.0 \cdot 10^{-3}$ in the second loop of Loading Condition (iii) and (iv), respectively. The special treatment made in the module works so that element shear stress becomes zero when reloading.

For Loading Condition (v), which corresponds to Patterns G and E, two loops of cyclic shear loading are applied like Loading Condition (iv), but the first loop is applied to the 2nd crack only. The resulting shear stress-shear strain is exactly the same as that of Loading Condition (iv), which is appropriate because Loading Condition (v) and (iv) are symmetrical.

Finally, we demonstrate the performance of the developed module to reproduce the shear loading test, comparing the results of E-FrontISTR with those of COM3. Figure 6 shows the shear strain-shear stress relation as shown in Fig. 2. The results show that the newly implemented model have a good accuracy with COM3.

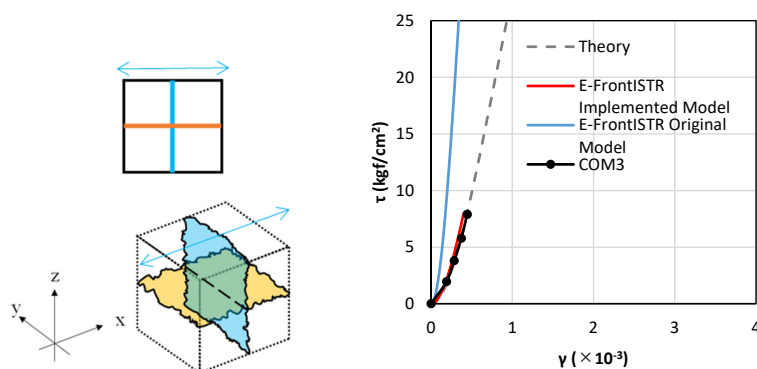


Figure 6. Comparative analysis of improved E-FrontISTR with COM3.

SIMULATION

FEM analysis is performed to reproduce results of RC shear wall experiments conducted at the Tadotsu Testing Laboratory of the Nuclear Power Engineering Corporation (NUPEC)⁹⁾. The numerical analysis model of the experiment specimen is shown in Fig. 7. An RC seismic wall is modeled using solid elements with RC nonlinearities, while the top slab, foundation slab, and additional weight are modeled using linear solid elements. The reinforcement bars of the seismic wall are placed between the solid elements as plane stress elements. Material parameters shown in Reference 5) are used.

A set of five input waves were used in the experiment. For a one-directional reference wave of 16 sec, five magnified waves, called RUN-1 to RUN-5, were used; the degree of the magnification was set according to the strain level of interest. In the numerical analysis, after the self-weight loading, five waves are input to the numerical analysis model. Time increment is 0.001 sec, which results in 16,000 time steps for each RUN and 80,000 time steps as the whole.

While the sequence of five magnified input waves induce considerably large nonlinearity in concrete, E-FrontISTR implemented with the developed module succeed to make stable numerical computation of 80,000 time steps. In particular, in the analysis of RUN-5 that uses strongest input wave, E-FrontISTR does not fail to produce converged solution for the nonlinear constitutive relation which reaches the ultimate capacity of multiply cracked concrete.

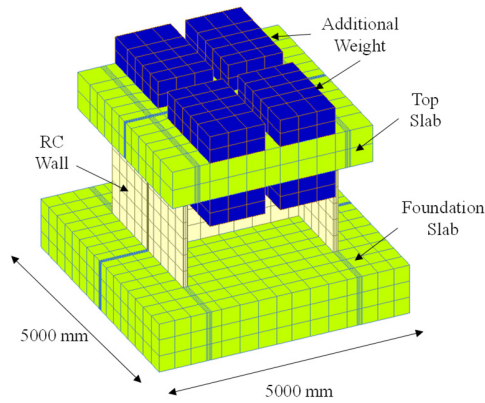


Figure 7. Analysis model of experiment specimen used in NUPEC test.

The acceleration time history for RUN-5 is shown in Figure 8. A significant difference cannot be seen for the E-FrontISTR implemented with the developed module, compared with original E-FrontISTR. However, it is seen that the agreement of the numerical analysis with the experimental data increases after 5.3 sec.

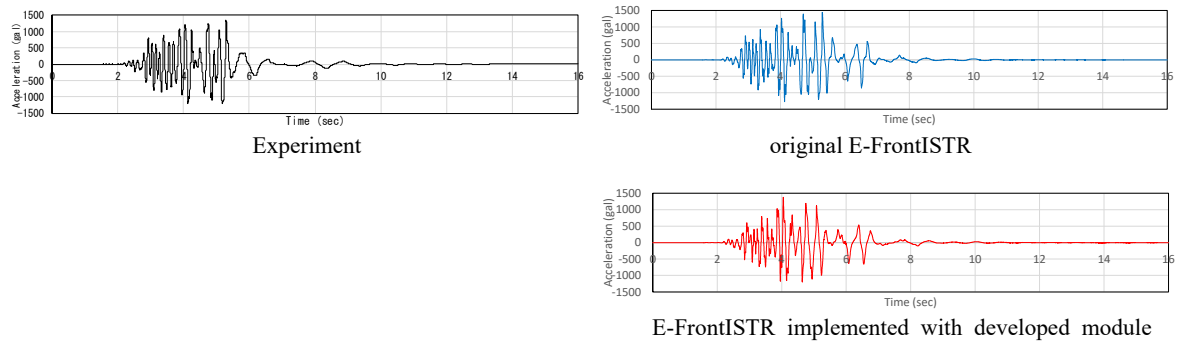


Figure 8. Acceleration time history for RUN-5.

To examine the details, we show the inertial force-displacement relation and the principal strain distribution in the web wall for RUN-5 in Figures 9. and 10. As for the inertial force-displacement relation, the developed module succeeds to reproduce softening behaviors better than the original E-FrontISTR. The results of E-FrontISTR with the developed module computes wider damaged parts which are evaluated from the principle strain. These parts correspond to severely cracked concrete observed in the experiment. While the original E-FrontISTR underestimates cracked concrete parts, the developed module does not.

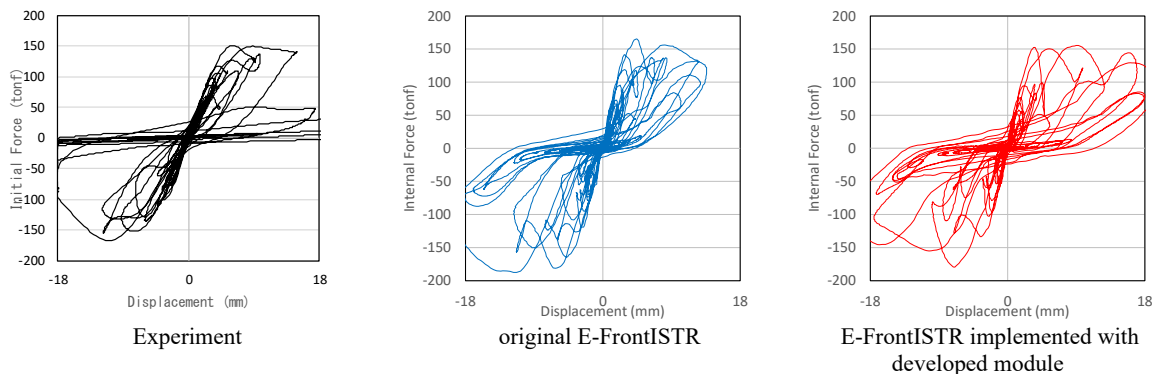


Figure 9. Inertial force-displacement relation for RUN-5.

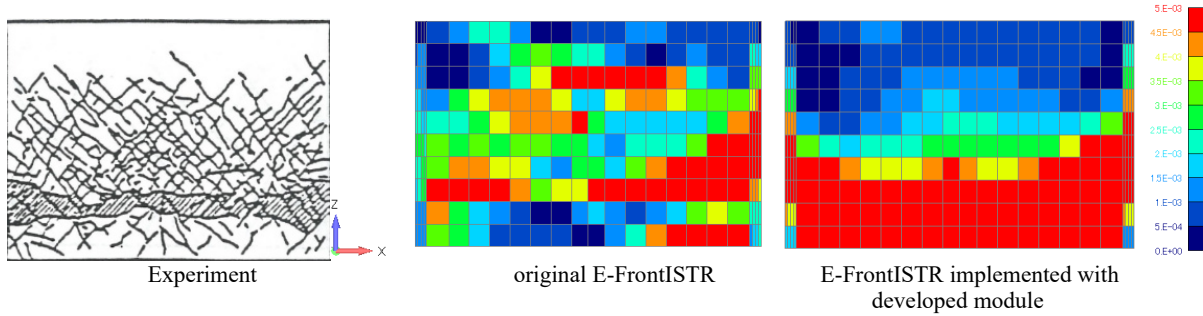


Figure 10. Principal strain distribution in web wall after RUN-5.

Figure 11. shows the time history of residual error and iterative number for nonlinear analysis of RUN-5. In this simulation, the maximum number of iterations until convergence in the nonlinear analysis was 100, and the convergence criteria for the residual error was $1.0 \cdot 10^{-3}$. Since the developed module has complicated patterns of loading states for multiple cracking, the convergence has slightly dropped for strong accelerations compared to the original module. However, since the developed module uses Eq. 8. or Eq. 10. for shear stiffness, the total number of nonlinear iterations is actually smaller than the calculation with the original module; 281,926 times compared to 415,724 times of nonlinear iterations.

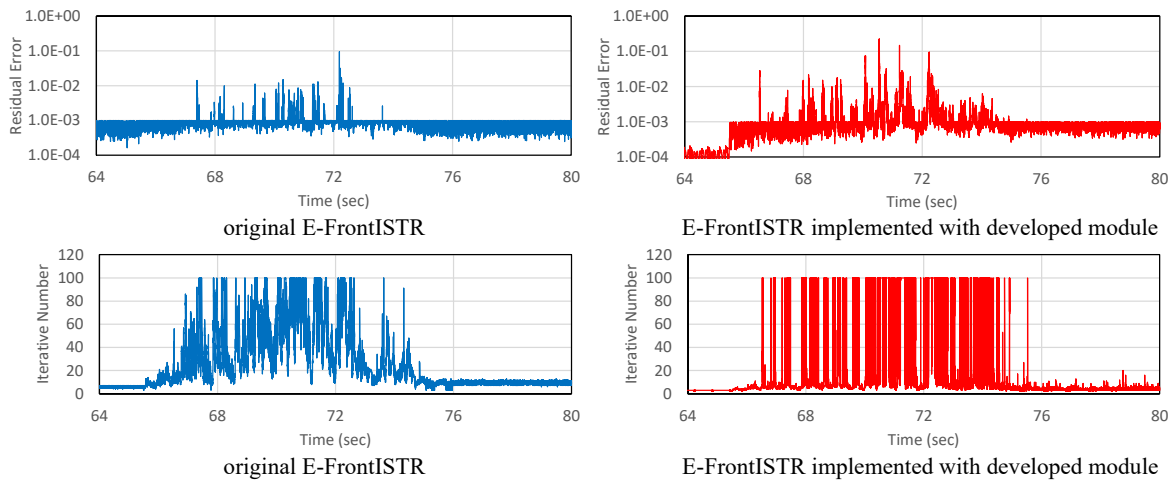


Figure 11. Time history of residual error and iterative number for RUN-5.

CONCLUSIONS

In this study, a module for the shear transfer mechanism is developed, to extend the applicability of E-FrontISTR to stronger ground motions which could induce multiple cracking in RC members of a nuclear power plant building. Most careful coding is needed because the three loading states of concrete results in numerous patterns of a set of loading states for multiple cracking. It also requires most careful verification of the developed module. For the case of two crack planes, the developed module succeeded to reproduce all eight patterns of loading states. It was shown in the numerical experiment using an RC building model that E-FrontISTR implemented with the developed module could make stable numerical computation even when multiple cracking takes place.

REFERENCES

- 1) DIANA FEA B.V. (2024). <https://dianafea.com/>.
- 2) Fukuura, N. and Maekawa, K. (1999). "Spatially averaged constitutive law for RC in-plane elements with non-orthogonal cracking as far as 4-way directions", *J Japan Soc Civil Eng*, 1999(634), 177-195.
- 3) Fukuura, N. (1998). "History-dependent constitutive model of reinforced concrete elements with cracks in four directions", Doctoral Thesis, University of Tokyo.
- 4) Maekawa, K., Okamura, H. and Pimanmas, A. (2003). *Non-Linear Mechanics of Reinforced Concrete*. Taylor & Francis.
- 5) Miyagawa, Y. (2019) "Development of a fragility evaluation program for reinforced concrete structures with parallel computer", Report of Central Research Institute of Electric Power Industry.
- 6) Motoyama, H., Sawada, M., Hotta, W., Haba, K., Otsuka, Y., Akiba, H. and Hori, M. (2021). 8"Development of a general-purpose parallel finite element method for analyzing earthquake engineering problems." *Earthquake Engineering and Structural Dynamics*, GBR, 50(15), 4180-4198
- 7) Motoyama, H. and Hori, M. (2019). Development and efficiency investigation of parallel computing seismic response analysis for high-fidelity model of large-scale reinforced concrete structures. Transactions SMiRT-25, Charlotte, NC, USA.
- 8) NEA: Seismic Shear Wall ISP NUPEC's Seismic Ultimate Dynamic Response Test, Comparison Report, NEA/CSNI/ R (96) 10, 1996.
- 9) Yamashita, T., Hori, M., Oguni, K., Okazawa, S., Maki, T. and Takahashi, Y. (2011). "Reformulation of non-linear constitutive relations of concrete for largescale finite element method analysis." *J Japan Soc Civil Eng*, JP, 67(1),145-154.